We are IntechOpen, the world's leading publisher of Open Access books Built by scientists, for scientists

6,900
Open access books available

185,000
International authors and editors

200M
Downloads

Our authors are among the

154
Countries delivered to

TOP 1%
most cited scientists

12.2%
Contributors from top 500 universities

CLARIVATE ANALYTICS

BOOK CITATION INDEX

INDEXED

WEB OF SCIENCE™

Selection of our books indexed in the Book Citation Index
in Web of Science™ Core Collection (BKCI)

Interested in publishing with us?
Contact book.department@intechopen.com

Numbers displayed above are based on latest data collected.
For more information visit www.intechopen.com

Development of PVA/Fe$_3$O$_4$ as Smart Magnetic Hydrogels for Biomedical Applications

Malik Anjelh Baqiya, Ahmad Taufiq, Sunaryono, Munaji, Dita Puspita Sari, Yanurita Dwihapsari and Darminto

Abstract

Polyvinyl alcohol (PVA)/Fe$_3$O$_4$ magnetic hydrogels had been fabricated by freezing-thawing (F-T) cycle technique, employing natural iron sand as the raw material for the magnetic micro- and nano-sized fillers. An exploration of the durability and magneto-elasticity as well as PVA hydrogel applications in the assessment of human brain tumor was also intensively conducted. The performance of the PVA and magnetic hydrogels mainly depends on the structural dynamic properties, such as polymeric crystallization and particle size. The durability of PVA/Fe$_3$O$_4$ magnetic hydrogels affecting the magnetoelasticity is determined by the concentration ratio of PVA and water, number of F-T cycles, and the concentration of Fe$_3$O$_4$ particles. By controlling those parameters, it was found that hydrogels had PVA: water ratio of 23:100 and four times F-T cycles possessed good mechanical properties. Due to the biocompatible character, the PVA hydrogel was used in the assessment of the human brain tumor, analyzed from the apparent diffusion coefficient (ADC) value representing the diffusion coefficient of a biological tissue. It was found that the abnormal tissue has a low ADC value compared with the normal one. Moreover, the higher b-value of the diffusion-weighted magnetic resonance imaging (DW-MRI) measurement is more preferred in obtaining a good contrast of the data imaging.

Keywords: PVA hydrogels, ferrogels, freezing-thawing method, magnetoelasticity, biomedical applications

1. Introduction

The hydrogel is one of the smart polymeric gels consisting of (physically or chemically) cross-linked polymer in water. Due to its hydrophobicity and biocompatibility properties, hydrogel

has been an interesting biomaterial used commonly for biotechnological applications [1–3] and drug delivery systems [4–6]. The physically cross-linked hydrogels can be constructed by hydrogen bonds, crystallization, and ionic and protein interactions, whereas the chemically cross-linked hydrogels can be built by complex chemical reaction (aldehydes), high energy radiation, polymerization, and enzymes [1, 7–9]. There is a disadvantage for the hydrogels prepared by the chemically cross-linked agent and gamma irradiation, namely a toxic residue that might be harmful to biological tissue. Therefore, the physically cross-linked hydrogels are more preferable to be applied for biomedical purposes [8]. Basically, hydrogels are sensitive to some environmental variables, such as acidity level (pH), temperature, electromagnetic signal, light, pressure, and other stimuli, so that they can be applied based on the proper environmental condition [10, 11]. A review of a particular number of synthetic hydrogels for biomedical applications and tissue engineering has been discussed [4, 12, 13].

Polyvinyl alcohol (PVA) is a biocompatible, water-soluble, and nontoxic synthetic polymer, which can be prepared to be a flexible material called PVA hydrogel. A physically cross-linked PVA hydrogel can be achieved by freezing-thawing (F-T) cyclic process [14, 15]. The networking gel structure, crystallinity, stability, and viscoelastic properties of the PVA hydrogels have been investigated [16–19]. The properties of PVA hydrogels prepared by F-T process depend on the molecular weight and concentration of the aqueous PVA solution, temperature, time duration, and number of F-T cycle processes [20]. For instance, Li and coworkers have successfully produced a reversible gel using poly(N-isopropyl acrylamide) (PNIPA) and polyacrylamide (PAM), which can be controlled by external stimuli such as temperature [21].

It has been found that cross-linking density and crystallinity of PVA hydrogel influence the overall mechanical properties of a hydrogel. Gupta et al. [22] had studied the effect of PVA concentration on both modulus elasticity and tensile strength of PVA hydrogel. They found that both mechanical properties increased with increasing PVA concentration up to 16% due to a higher degree of crystallinity and developing hydrogen bond interaction in the PVA hydrogel. In contrast, it has also been shown that higher crystallinity of the hydrogel (obtained by increasing PVA concentration) may cause the increase of optical contact angle, indicating the decrease of water affinity [23]. This is one parameter that should be concerned for producing a stable PVA hydrogel. Moreover, it is revealed that the number of cyclic processes in the F-T method affects the degree of cross-linking density. A higher number of repeated cycle results in the decrease in the amount of not incorporated PVA in the networking structure of hydrogel meaning that the polymer chains of PVA are dispersed and unrelated each other [24].

In the tissue engineering, a transparent PVA hydrogel has been successfully developed as soft tissue substitution due to the similar microstructure and mechanical properties to that of the biological cells and organs [25]. PVA-based composite gels have been also intensively studied for wound healing, tissue replacement, and magnetic-controlled drug delivery devices [26–28]. Liu et al. [29] have demonstrated PVA hydrogel produced by the F-T process as one of the potential materials for an artificial blood vessel. Furthermore, the F-T process can be used widely for preparing and storing cell-laden hydrogels with adjustable mechanical properties [30].

One important key for organ replication in tissue engineering is a complete knowledge of microscopic, physical, and chemical properties based on the desired organ. Recent development of hydrogel technologies for mimicking natural tissue has been briefly reviewed [31]. It is crucial for constructing a tissue from hydrogel without causing significant cell damage. Investigation on a transparent PVA hydrogel as tissue-equivalent material in the surgical application has been conducted [32]. They have found that PVA hydrogels could be applied for a suitable substitution for soft tissue accuracy and surgical purposes. Forte et al. [33] have successfully developed a composite hydrogel (PVA hydrogel) to mimic brain tissue. They tried to vary the PVA concentration in order to tune the mechanical response of brain tissue within a wide range of stress/strain and testing conditions. In the brain tissue replica, it is important to study accurately the brain shift phenomenon between the abnormal and the normal one.

2. Magnetic hydrogels (Ferrogels) and their physical properties

The magnetic hydrogel, or so-called ferrogel, is one of the "smart" polymeric composite gels containing micro- or nano-sized magnetic particles as filler in its polymeric matrix. There are some magnetite hydrogels (ferrogels) that have been successfully developed recently, namely PVA-Fe$_3$O$_4$-based hydrogel [34], Fe$_3$O$_4$-polyacrylamide (PAM) hydrogels [35], and Fe$_3$O$_4$-polymethylmethacrylate (PMMA) hydrogels [36]. They have found that those magnetic nanocomposites forming magnetic hydrogels have superparamagnetic behavior due to the presence of dispersed magnetic nanoparticles in the polymeric matrix. The properties of superparamagnetic of magnetic iron oxide nanoparticles itself have been investigated intensively [37]. A simulation study of deformation, elasticity, and magnetic response of magnetic nanoparticles cross-linked in a gel (polymeric matrix) has been conducted [38]. They have found that the degree of networking chains plays an important role in determining the stiffness and magnetosensitivity of the magnetic hydrogels. The sensitivity of magnetic response in the external magnetic field depends strongly on the volume fraction of both magnetic nanoparticles and polymeric base matrix influencing the interacting energy in the ferrogel [28]. They found an optimum magnetosensitivity with Fe$_3$O$_4$ and PVA concentration in the range of 17–34% and 10–12.5%, respectively.

Ferrogel is a new type of polymeric matrix composites, in which they are physically (or chemically) cross-linked polymer network containing dispersed magnetic particles. Zrínyi et al. [39] have synthesized ferrogel as a new promising material for magnetic-responsive applications. Ramanujan and Lao [40] and Reséndiz-Hernández et al. [41] have developed composite gels based on PVA and magnetite (Fe$_3$O$_4$) particles by conventional F-T process. Moreover, Hernández et al. [19] have reported the viscoelastic properties of PVA hydrogel and ferrogel prepared by F-T cyclic process. It has been revealed that the reinforcement effect from the magnetic particles, as well as the mechanical properties, of the PVA-Fe$_3$O$_4$ ferrogels depends on the size, possible agglomeration, and concentration (volume fraction) of the magnetic particles [42]. It has been noted that the concentration of Fe$_3$O$_4$ nanoparticles affects the thermal

stability of the ferrogels [43]. As for the mechanical properties of the PVA-Fe$_3$O$_4$ ferrogels, it has been shown that the deflection and elongation parameters are dependent on the Fe$_3$O$_4$ concentration and external magnetic field strength [40] and the deformation is independent on the shape of ferrogels [44]. Experimentally, the magnetodeformation of the ferrogels with highly concentrated particles (approximately above 30%) is due to the effect of short range order and magnetic interaction among the particles [45, 46]. Furthermore, the structural and magnetic behavior of ferrogels has been intensively studied with the dispersed magnetic particle having average size less than 10 nm [47, 48].

Sunaryono et al. have shown that the hydrogels owing the threshold PVA concentration of 23% in water content have the best mechanical properties [49]. Moreover, the lower Fe$_3$O$_4$ concentration has been found to be responsible for a weak magnetic response due to the increase of particle free volume and the decrease of interaction energy between magnetic nanoparticles and the cross-linked PVA hydrogel [48]. However, Sunaryono et al. [48, 49] stated a crucial problem is related to the durability of the PVA hydrogels and ferrogels prepared by F-T cyclic process.

In this chapter, at first, we provide a study of PVA hydrogel application in tissue engineering. Then, it is continued by investigation of the durability of ferrogels prepared by F-T cyclic process. Finally, the structural and magnetic properties of ferrogels are discussed briefly.

3. Fabrication and characterization of PVA hydrogel

The PVA polymeric powder (Mw = 60,000 g/mol, Merck Schuchardt OHG, Germany) with a degree of hydrolysis ≥98% was used for PVA solution. PVA hydrogels were fabricated by F-T cyclic process. First, the PVA polymer was dissolved in distilled water with a variation of weight compositions, namely 7.5, 10, 12.5, and 15 wt%. The solution was mixed and heated at 70–90°C to improve the solubility of the PVA polymer in water, as suggested in the previous papers [48, 50, 51]. Once the mixture was perfectly dissolved, indicated by a physical change from liquid to paste, it was then loaded into a cylindrical plastic mold followed by F-T process. The solution was cooled and kept at the frozen state at –10°C for 3 h. The process was continued by thawing at room temperature for 1 h. This F-T process was repeated to obtain PVA hydrogel samples up to five cycles. The PVA hydrogel samples were also prepared by varying the composition ratio of PVA and water as mentioned earlier.

The 1.5-T scanner (Signa Horizon; GE Medical Systems, Milwaukee, WI, USA) was used for the study of diffusion-weighted magnetic resonance imaging (DW-MRI). Apparent diffusion coefficient (ADC) value was obtained from MRI with diffusion-weighted imaging (DWI) method following Stejskal-Tanner sequence. The ADC value was calculated by Functool software (GE Medical Systems) for each sample. The characterization steps were similar to the previous reports [50, 51].
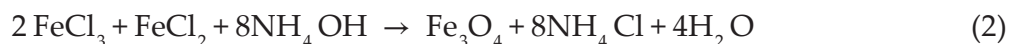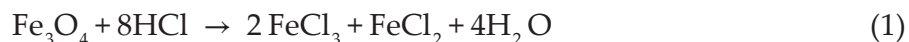
The consistency measurement was conducted using a penetrometer (Precision 73,515, Petroleum Analyzer Co., San Antonio, TX, USA) using a pressure sensor. The penetrometer

was set under gravity force for 5 s, and the depth of penetration was measured in tenths of millimeters. The depth of penetration depended on the kinetic energy applied to the penetrometer and the sample resistance. The resistance data were collected to obtain the consistency value describing the required mechanical force to decelerate from its initial velocity to zero velocity.

4. Preparation of Fe_3O_4 nanoparticles from iron sand

Fe_3O_4 nanoparticles were prepared by coprecipitation method employing natural iron sand as a raw material. The preparation was the same as explained in the former papers [48, 52]. First, iron sand was extracted by permanent magnet several times to obtain microsized Fe_3O_4 powders. HCl and NH_4OH were used as dissolving and precipitating agents, respectively. Fe_3O_4 nanoparticles produced by the coprecipitation method were based on the following chemical reaction [52, 53].

$$Fe_3O_4 + 8HCl \rightarrow 2FeCl_3 + FeCl_2 + 4H_2O \tag{1}$$

$$2FeCl_3 + FeCl_2 + 8NH_4OH \rightarrow Fe_3O_4 + 8NH_4Cl + 4H_2O \tag{2}$$

Both reactions were maintained at room temperature. A complete reaction was indicated by the color change of the solution and the formation of black precipitation. Finally, the precipitated powders were rinsed several times using distilled water and then dried at 100°C for 1 h for ferrogel fabrication.

5. Fabrication and characterization of PVA/Fe_3O_4 hydrogel (Ferrogel) based on iron sand

Ferrogel was fabricated by distributing the prepared Fe_3O_4 nanoparticles in the PVA hydrogel paste solution, and then, they were stirred to obtain a uniform gel. Furthermore, the mixture gel was placed into a cylindrical mold to perform the similar F-T cyclic process as in the PVA hydrogels fabrication. The ferrogel samples were prepared by varying the concentration of PVA and Fe_3O_4 nanoparticles, as well as the number of F-T cycles.

Basic characterizations using X-ray diffractometer (XRD) and transmission electron microscopy (TEM) were conducted to analyze the crystal structure and particle morphology of Fe_3O_4 nanoparticles and ferrogels, respectively. Vibrating sample magnetometer (VSM) and superconducting quantum interference device (SQUID) measurements were taken to investigate the magnetic properties of the PVA ferrogels. Particle size and the distribution of Fe_3O_4 nanoparticles in the PVA hydrogels were analyzed using small-angle X-ray scattering (SAXS) instrument as in the reported paper [48].

The ferrogels were exposed to the external magnetic field of an electromagnet apparatus, which is able to generate a magnetic field up to 460 mT. The response of the ferrogel was measured by the extent of deflection and elongation. The top end of a ferrogel sample was fixed, whereas the lower end was free to deflect and elongate during the application of the external magnetic field. Variation in the magnetic field was obtained by changing the electric current of the electromagnetic apparatus. The Young's modulus was measured using a universal mechanical tester.

6. Applications of PVA hydrogels for tissue engineering

PVA hydrogels fabricated through a number of F-T cycle processes have the ability to mimic a complex structure of human body. In a normal condition, water can be diffused into organic tissue during body's metabolism. However, the diffusion of water can be disturbed if water molecules are passing through an abnormal tissue due to swelling of the tissue, for example in tumor tissue. Moreover, about two-thirds of the human body consist of water, in which water molecules have hydrogen atoms that allow for magnetic resonance imaging (MRI) observation. Diffusion-weighted MRI (DW-MRI) is a device with high sensitivity in detecting "Brownian motions." The diffusion of water molecules caused by heat energy associated with the temperature of the human body can be used for analyzing a variety of brain diseases including brain tumors [54]. Additionally, diffusion-weighted imaging (DWI) is a technique that can be used to measure diffusion of water molecules in biological tissue such as white matter in the brain. In the MRI observation, the value of apparent diffusion coefficient (ADC) is used widely for describing the diffusion coefficient of the material.

In order to investigate the diffusion properties and the consistencies of the fabricated PVA hydrogels applied for tissue replica, several PVA hydrogel samples have been produced by variation number of F-T cycles and PVA concentrations. ADC values of the PVA hydrogels were obtained by performing the DW-MRI measurement. Sari et al. [51] have shown the ADC values versus PVA concentration for PVA hydrogels with the F-T process of three to five cycles. It has been found that the increase of PVA concentration from 7.5 to 15 wt% decreases the ADC values corresponding to the diffusion coefficient of all PVA hydrogels.

The enlargement of the tumor cells causes a reduction in the volume of extracellular space, increases the intracellular viscosity, and then inhibits the movement of water molecules described by the decrease of ADC value. Moreover, for PVA hydrogel fabricated by cryogelation process, the decrease of ADC value is described by swelling indicated by the significant increase of crystallization of hydrogel with increasing the number of F-T cycles. ADC value helps to distinguish a tumor tissue from a nontumor tissue. However, the abnormal tissue of brain tumor has a variety of classifications depending on the location and type of tumor tissue. Therefore, in the application of DW-MRI, it is necessary to find the most aggressive area at first to identify the highest cellularity and the most restrictive for the movement of water molecules. The use of higher b-value is to obtain a brighter contrast and has the impact on the easiness of diffusion imaging. The higher b-value can produce images on the high value of signal-to-noise ratio (SNR). Otherwise, at 1.5 T or lower, a low b-value may produce a poor image quality and lower value of SNR [55].

Figure 1 displays the ADC values of the PVA hydrogels measured from DW-MRI with b = 1000 and 3000 s/mm^2 as a function of F-T cycles and different PVA concentration. It has been found that the greater the concentration and number of cycles, the lower the diffusion coefficient of the PVA hydrogels. The crystallization, the degree of the physically cross-linked network, and the stiffness of hydrogel increase with the increase of the F-T cycle [15, 56]. The increase of crystallization indicates that the diffusion of water may be inhibited, so that the value of diffusion coefficient, described by ADC value, decreases. This is general diffusion behavior of a hydrogel, in which the diffusivity of a hydrogel decreases as cross-linking density increases and as the volume fraction of water within the hydrogel decreases [57]. It has also been indicated that the linearity of the ADC value as a function of F-T cycles at b = 3000 s/mm^2 is better than that at b = 1000 s/mm^2. This result is in a good agreement with the former result [55].
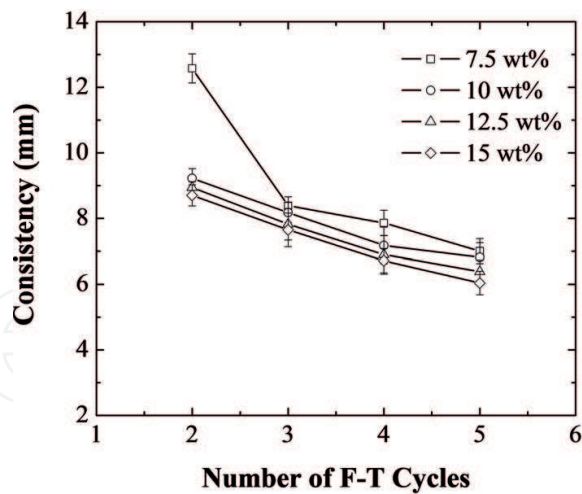
Figure 2 shows the consistency measurement as a function of F-T cycles and different PVA concentration. The data show that the higher PVA concentration and a number of F-T cycles cause the lower consistency and ADC value [50]. These results are consistent with the former paper [58]. The Pearson correlation method was used to correlate the data and are presented in **Table 1**. It is shown that the average value of ADC at b = 3000 s/mm^2 is good and slightly smaller than that at b = 1000 s/mm^2. The data have a good correlation (correlation number of 0.92—0.99), so that it can assess the abnormal tissue consistency [51].

Generally, ADC values of the human brain for both normal and abnormal cases are different significantly. In the DW-MRI analysis, ADC value in the normal human brain is about 0.75 mm^2/s and the higher b-value results in the lower ADC value. A tissue having low ADC value eliminates signals faster than that on the tissue having higher ADC value, and therefore, the contrast should increase. Sari et al. [51] have analyzed some cases for human brain tumor from the DW-MRI images at b-value of 1000 and 3000 s/mm^2. They also found that the tissue having low ADC value indicates lower consistency or harder than the tissue having high ADC value. The ADC measurement using b = 1000 s/mm^2 can distinguish the harder tissue with the
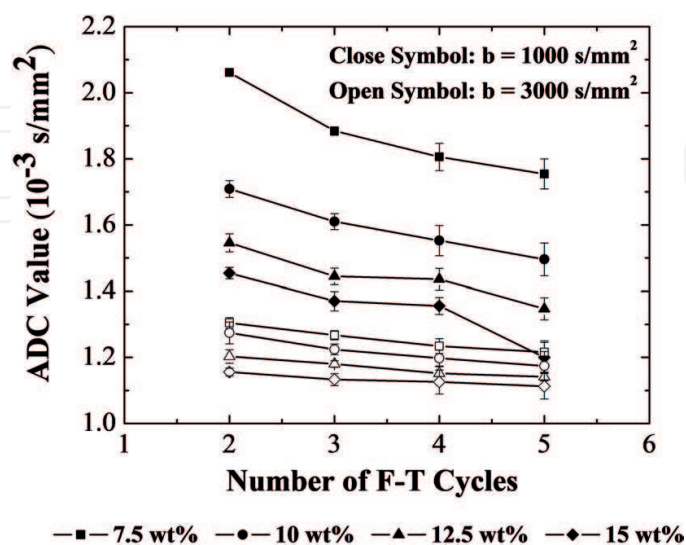
Figure 1. ADC value of PVA hydrogels on the DW-MRI at b-value of 1000 s/mm^2 (closed symbols) and 3000 s/mm^2 (opened symbols) as a function of the number of F-T cycles and PVA concentration.

Figure 2. Consistency measurement using digital penetrometer as a function of the number of F-T cycles and PVA concentration.

normal one and provides a clearer image, although the ratio of normal and abnormal tissue is not as high as the use of b = 3000 s/mm^2. A better value of correlation with the physical parameters gives a suggestion that the use of DW-MRI 1.5 T with b = 1000 s/mm^2 provides a better image and the use of penetrometer is necessary for additional information for determining surgery. Otherwise, the use of DW-MRI 1.5 T with b-value higher than 1000 s/mm^2 is more preferred to examine the swelling that occurs around the area of the abnormal tissue because it provides more contrast image.

PVA hydrogels with different F-T cycle at constant PVA concentration of 10 wt%	Data (s/mm^2)	
	b = 1000	b = 3000
Two cycles	0.96	0.77
Three cycles	0.96	0.99
Four cycles	0.99	0.96
Five cycles	0.96	0.97
PVA hydrogels with different PVA concentration at constant F-T cycle for three times	Data (s/mm^2)	
	b = 1000	b = 3000
7.5 wt%	0.98	0.93
10 wt%	0.99	0.99
12.5 wt%	0.94	0.99
15 wt%	0.92	0.98

Table 1. The Pearson correlation result for both data of PVA hydrogels with different F-T cycle and PVA concentration.

7. Stability and durability of PVA-Fe$_3$O$_4$ hydrogels (Ferrogels)

In order to study the stability and durability of ferrogel, a number of ferrogel samples have been fabricated with a variation of PVA and water ratio, the concentration of Fe$_3$O$_4$ nanoparticles, and a number of F-T cycles. The stability was investigated by observing the increase of the required external magnetic field to elongate and deflect the ferrogels until a certain length and distance over a particular time. The observations were conducted from the first day since the ferrogels fabricated until the fifth day. The ferrogels can be called relatively stable if the change of required magnetic field is considerably small over the time to get the same deformation condition.

Table 2 shows ferrogel samples with a variation of PVA and water ratio together with their elasticity moduli. It can be seen from the elasticity properties that the stiffness of ferrogel depends on the PVA concentration in water. Higher PVA concentration causes the increase of stiffness. The stability of ferrogels is shown in **Figure 3**. **Figure 3** demonstrates the time dependence of the required external magnetic field to elongate ferrogel up to 1 mm. It indicates that

No.	Ratio of PVA and water	Fe$_3$O$_4$ (wt%)	Number of F-T cycles	Sample code	Modulus elasticity (Pa)
1	13:100	10	4	PA.13	67.18
2	18:100	10	4	PA.18	69.96
3	23:100	10	4	PA.23	61.23
4	28:100	10	4	PA.28	119.10
5	33:100	10	4	PA.33	221.20

Table 2. Ferrogel samples prepared with different PVA and water ratio, together with the modulus elasticity.
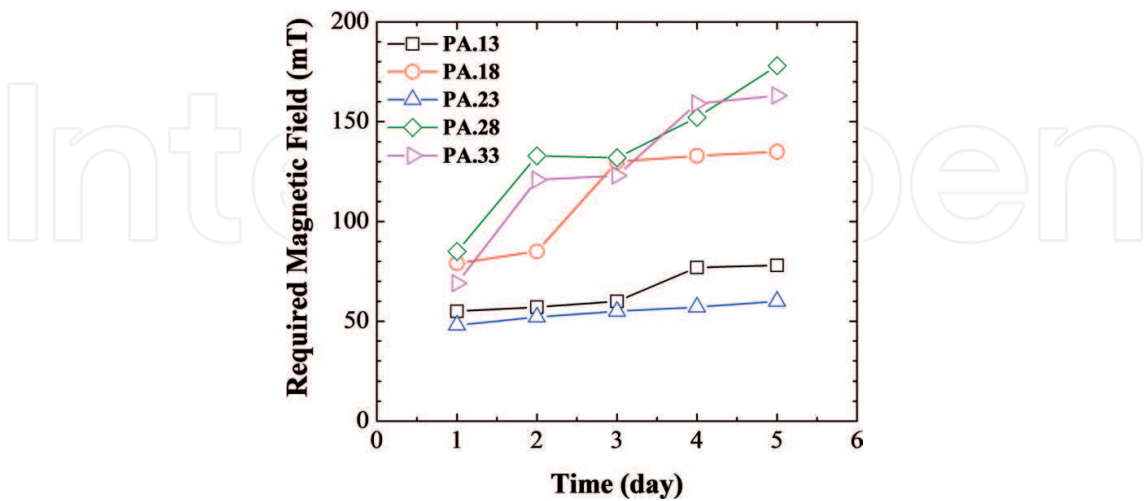
Figure 3. Required magnetic field to elongate ferrogel up to 1 mm as a function of time for ferrogels with different PVA and water ratio.

ferrogel becomes stiffer with the passage of time due to the decrease of water content. The ferrogel with PVA and water ratio of 23:100 (PA.23) shows a relatively small change of the required magnetic field up to five days indicating a relative stability compared to the others. This stability relates to the optimum portion of water inclusion binding in the PVA hydrogel.
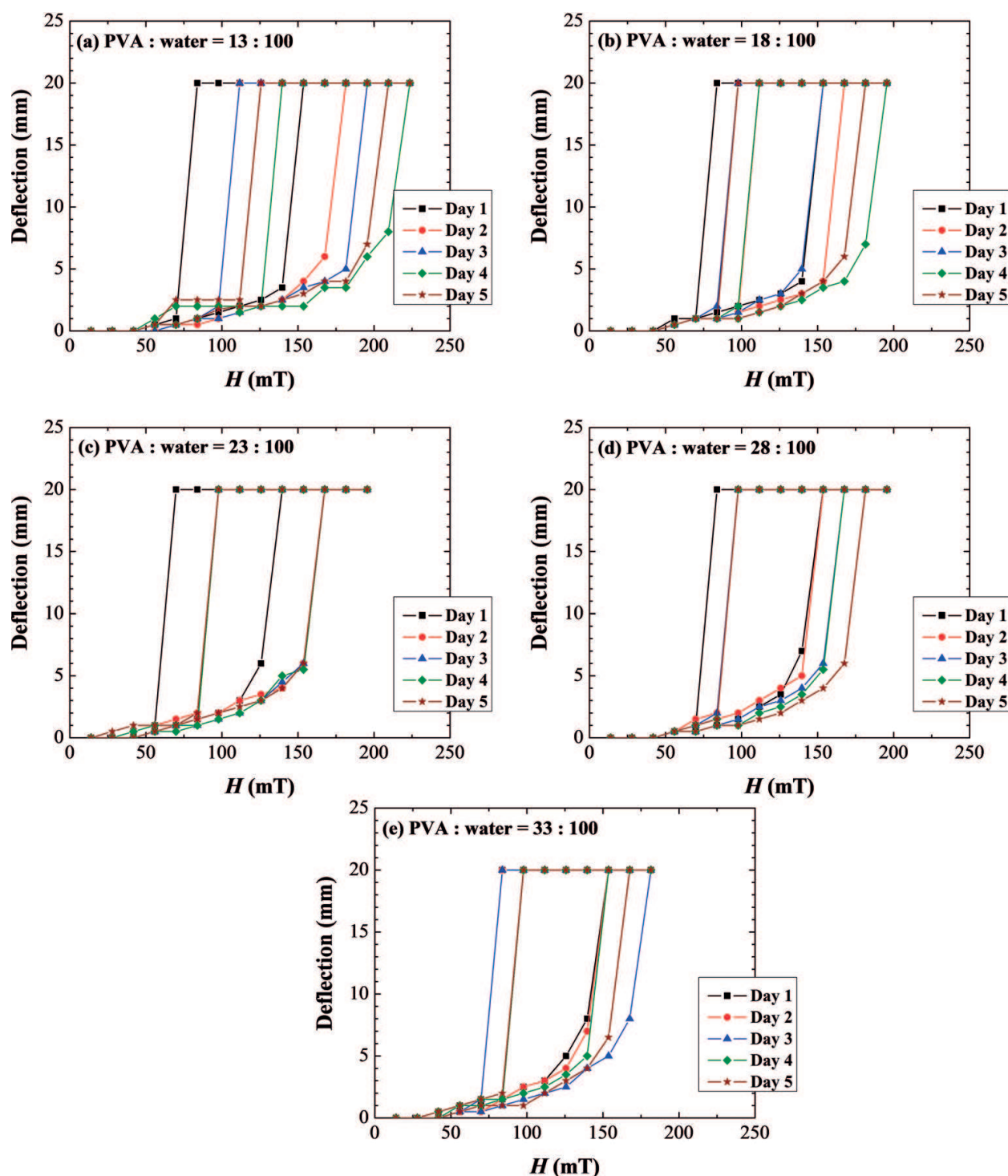
Figure 4. Hysteresis curves of the deflection behavior of ferrogels with PVA and water ratio: (a) 13:100, (b) 18:100, (c) 23:100, (d) 28:100, and (e) 33:100.

Figure 4 presents magnetic field dependence of ferrogel deflection with different PVA and water ratio. **Figure 4** displays interesting hysteresis loop in which the deflection increases with increasing magnetic field and returns to its original length through a different path, thereby decreasing the magnetic field. These noncontinuous deflection behaviors have also been observed by Zrínyi et al. [59] and modeled by Snyder et al. [60]. The hysteresis loops tend to shift day by day, indicating a rigid gel character due to the decrease of water content.

Ferrogels with different concentration of Fe$_3$O$_4$ nanoparticles and the modulus elasticity are presented in **Table 3**. It appears that there is no significant change in the modulus of elasticity with the increase of Fe$_3$O$_4$ concentration from 5 to 12.5 wt%. This result is consistent with the former report [40], in which the obtained elastic modulus was in the range of 0.17–0.75 MPa for a magnetoactive elastomer. **Figure 5** shows the stability characteristic of the ferrogels with various Fe$_3$O$_4$ concentrations associated with **Table 3**. It implies that the increase of nano-sized Fe$_3$O$_4$ concentration tends to decrease the required magnetic field to elongate ferrogel up to the same length for each day, indicating the decrease of water content and stiffer ferrogels. Ferrogel with Fe$_3$O$_4$ concentration of 10 wt% (FP.10) appears to be moderately stable compared to the others. For the ferrogels with Fe$_3$O$_4$ concentration less than 10 wt%, the trapped magnetic particles in the PVA chain were less and therefore the distribution was inhomogeneous, creating more spaces which were filled with water. According to the structural model of hydrogel described by Goiti et al. [43], the trapped, free and linked water molecules attached to the PVA chain may cause a soft ferrogel and dry quickly due to rapid evaporation of the water. On the other hand, for ferrogels with Fe$_3$O$_4$ concentration more than 10 wt%, there might be a space filled by Fe$_3$O$_4$ nanoparticles so that the water is suppressed. The Fe$_3$O$_4$ nanoparticles could directly coincide with the polymer chain. For the ferrogel with Fe$_3$O$_4$ concentration of 10 wt%, it is expected to have a proportional amount of solids and liquid, resulting in a good cross-linked hydrogel and then the trapped water can maintain flexibility of the gel.

Figure 6 shows magnetic field dependence of ferrogel deflection with different concentration of Fe$_3$O$_4$ nanoparticles. The hysteresis behavior of the deflection curves depends on the concentration of Fe$_3$O$_4$ nanoparticles and the elasticity of ferrogel itself. It should be noted that the hysteresis behavior observed in ferrogel is not consequences from the magnetic particles [59]. It appears that ferrogels with Fe$_3$O$_4$ concentrations of 10 and 12.5 wt% have no significant change in the hysteresis loops up to the fifth day. The change and the distortion

No	Ratio of PVA and water	Fe$_3$O$_4$ (wt%)	Number of F-T cycles	Sample code	Modulus elasticity (Pa)
1	23:100	5	4	FE.5	60.54
2	23:100	7.5	4	FE.7	60.94
3	23:100	10	4	FE.10	61.23
4	23:100	12.5	4	FE.12	61.59

Table 3. Ferrogel samples prepared with different Fe$_3$O$_4$ concentrations, together with the modulus elasticity.

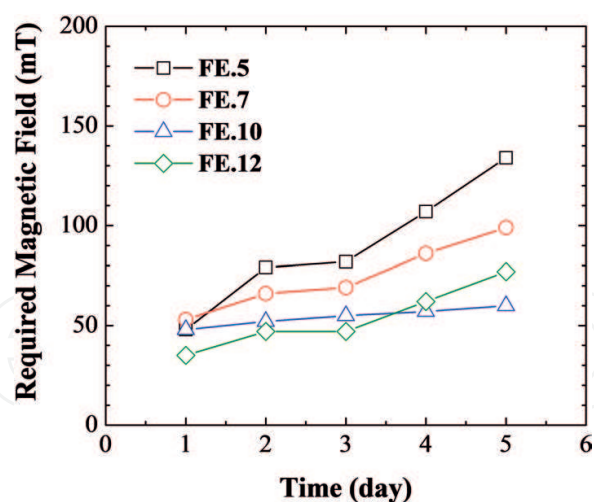**Figure 5.** Required magnetic field to elongate ferrogel up to 1 mm as a function of time for ferrogels with different Fe_3O_4 concentrations.

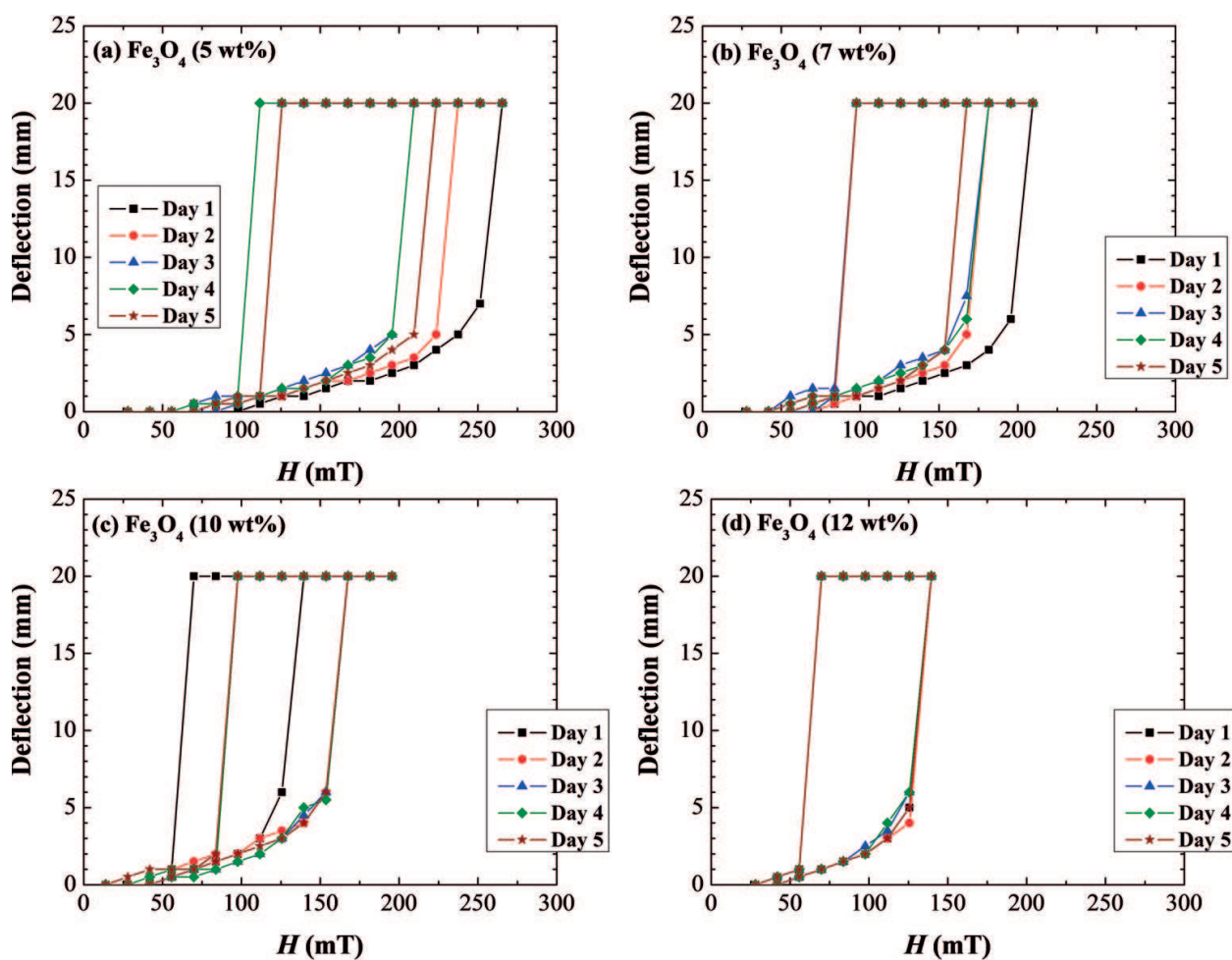**Figure 6.** Hysteresis curves of the deflection behavior of ferrogels with Fe_3O_4 concentration of: (a) 5 wt%, (b) 7 wt%, (c) 10 wt%, and (d) 12 wt%.

| No	Ratio of PVA and water	Fe$_3$O$_4$ (wt%)	Number of F-T cycles	Sample code	Modulus elasticity (Pa)
1	23:100	10	4	FT.4	61.23
2	23:100	10	8	FT.8	535.2
3	23:100	10	12	FT.12	267.0

Table 4. Ferrogel samples prepared with a different number of F-T cycles, together with the modulus elasticity.

of hysteresis shape are influenced by magnetostatic and magnetostriction mechanisms in the ferrogel [61]. Sample geometry may also be one parameter for determining the mechanical behaviors (elongation, deflection, etc.) of the ferrogel in the external magnetic field [60].

The modulus elasticity of ferrogels with a different number of F-T cycles was also investigated as shown in **Table 4**. In general, the greater the number of F-T cycles, the more rigid ferrogels will be obtained due to the evaporation of water. **Figure 7** shows the durability of ferrogels produced by 4, 8, and 12 times F-T cycles. It is also clear that ferrogel produced by four times F-T cycles has better stability as indicated by relatively small changes of the external magnetic field required to elongate ferrogel up to the same length until the fifth day. The stability of the ferrogels can also be studied by observing the hysteresis loop of elongation as shown in **Figure 8**. Ferrogels fabricated by more than four cycles are generally unstable, implying that there is a reduction of water in the ferrogels during F-T cycle processes. This result is consistent with the previous papers [34, 49]. Through the F-T cycles, crystallites will be formed and act as the cross-linking points in the polymer matrix. The amount and size of these crystallites depend on the number of F-T cycles, as well as composition and concentration of the initial solution [15].
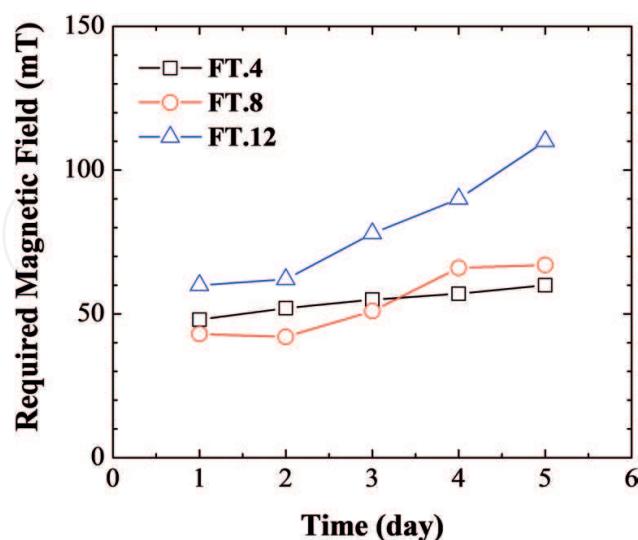
Figure 7. Required magnetic field to elongate ferrogel up to 1 mm as a function of time for ferrogels with a different number of F-T cycles.
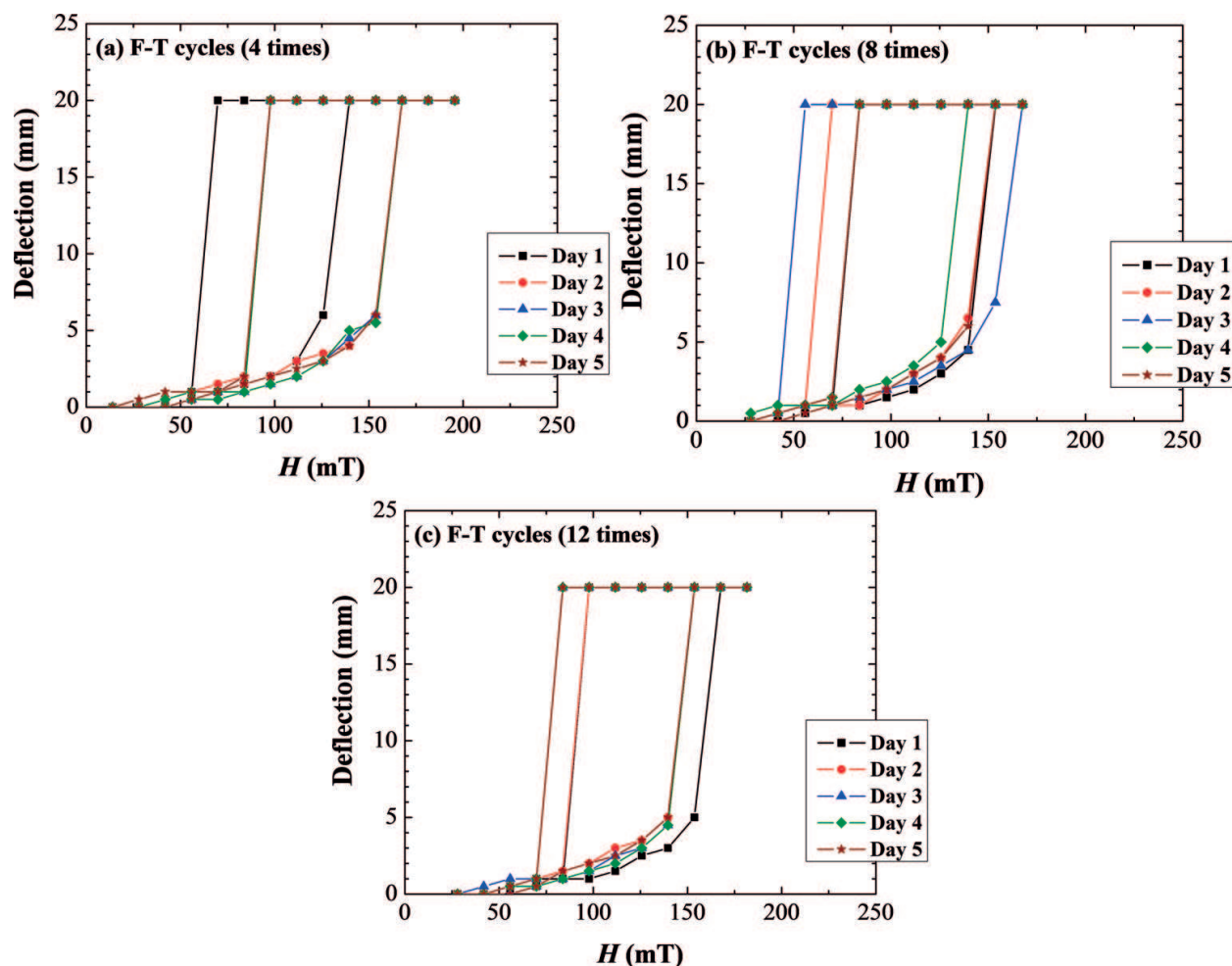
Figure 8. Hysteresis curves of the deflection behavior of ferrogels with the number of F-T cycles for: (a) 4, (b) 8, and (c) 12 times.

8. Structural and magnetic properties of Ferrogels

In addition to the substantial biomedical and biomechanical applications of PVA hydrogels and ferrogels, respectively, a basic study of structural and dynamical properties of ferrogel has to be investigated in detail. Structural studies using small-angle X-ray scattering (SAXS) measurement of PVA hydrogel and ferrogel have been reported by Puspitasari et al. [62] and Sunaryono et al. [48], respectively. Puspitasari et al. have confirmed that the crystallization of PVA hydrogel has a radius of approximately 2.9–3.3 nm and an average distance between polymer crystallites of 15–17.5 nm [62]. This result is consistent with the recent paper [48]. Moreover, Sunaryono et al. have illustrated the size distribution of Fe_3O_4 nanoparticles in the PVA hydrogel obtained by F-T cyclic process [48]. They have found that there are so-called primary particles (approximately 3 nm) and secondary particles as well as the clusters of magnetic nanoparticles in ferrogel observed by the synchrotron radiation (SAXS technique) with global fitting analysis data. The cluster size of the Fe_3O_4 in the ferrogel system was observed to be significantly reduced with decreasing concentration of the magnetic nanoparticles.

Ferrogel has potential application for an artificial muscle or a soft actuator due to the combined properties of good elasticity and flexibility from PVA hydrogel and specific magnetic behavior from the magnetic particles. Ramanujan et al. [40] have proposed two possible approaches of an artificial finger synthesized from PVA hydrogel and microsized iron oxide. First, they found that the deflection of ferrogel can be controlled by adjusting the concentration of magnetic particles. The second one is by coating manipulation of ferrogel. They demonstrated a finger-like motion based on instantaneous elongation and defection under external magnetic field.

As mentioned previously, in order to apply the ferrogel as an artificial tissue, one should understand the behavior of magnetoelastic properties. Based on numerous references [40, 48], the magnetoelasticity of ferrogel basically depends on the particle size and concentration of the magnetic particles in the polymeric matrix. Due to the particle size effect, the magnetization of microsized Fe$_3$O$_4$ particles in the ferrogel is generally higher than that of the nano-sized one. This may affect the threshold value of the magnetic field which is the minimum magnetic field required to start a large and instantaneous elongation or deflection of ferrogel. **Figure 9** shows the dependence of Fe$_3$O$_4$ concentration on the threshold magnetic field for both elongation and deflection of ferrogels with micro- and nano-sized Fe$_3$O$_4$ particles. It is found that the threshold magnetic field tends to decrease with increasing concentration of Fe$_3$O$_4$ particles. This result is consistent with the former report [40]. This result implies that the ferrogels are more sensitive to the external magnetic field with the increase of Fe$_3$O$_4$ concentration. **Figure 9** reflects the magnetic response for both variation of ferrogels, in which the ferrogel with microsized Fe$_3$O$_4$ particles has smaller threshold value than the ferrogel with nano-sized Fe$_3$O$_4$ particles as a consequence of the higher magnetization.

Figure 10 displays the Fe$_3$O$_4$ concentration dependence of elongation and deflection behaviors for both ferrogels with micro- and nano-sized Fe$_3$O$_4$ particles as fillers. It indicates that ferrogel with microsized filler is more sensitive to deform ferrogel under external magnetic field. This result can be explained by the lower threshold value of the magnetic field as illustrated in **Figure 9**. **Figure 11** shows the magnetoelastic hysteresis loops for ferrogels with different
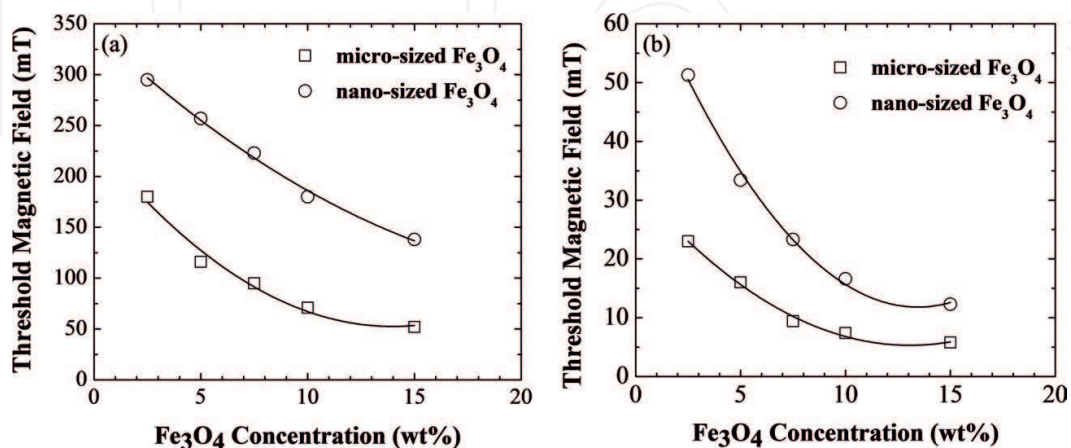

Figure 9. The threshold of magnetic field versus micro- and nano-sized Fe$_3$O$_4$ fillers for ferrogels during (a) elongation and (b) deflection. The solid lines are for the eye guidance.
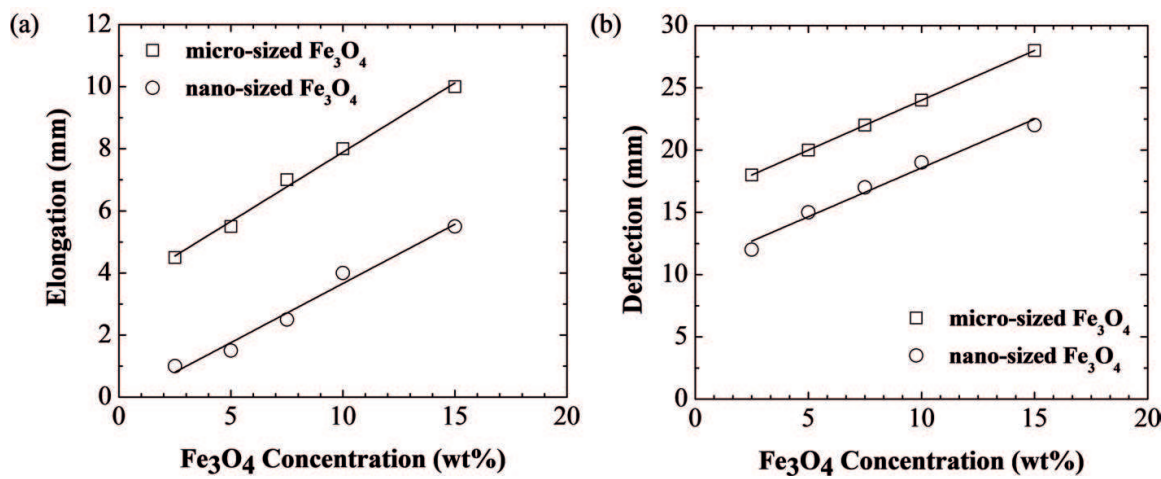
Figure 10. (a) Elongation and (b) deflection of ferrogels under 329 mT versus the concentration of micro- and nano-sized Fe₃O₄ particles as fillers. The solid lines are for the eye guidance.

concentration of microsized Fe₃O₄ particles from 2.5 to 15%. The hysteresis loops are found to be narrower and smaller with decreasing magnetic filler concentration. This is attributed to the different magnetic response of ferrogel to be deformed and returned to its original length and position. This behavior is also associated with a magnetic remnant of the ferrogels. A higher magnetic concentration leads to a higher ferrogel ability to deform even under a low external magnetic field. Moreover, a wider hysteresis loop for ferrogel with microsized filler was observed, indicating a stronger magnetic saturation. This is in a good agreement with the previous paper [27] that the ferrogel with large particle size has the best magnetosensitive effect, so it can be applied for drug release system.
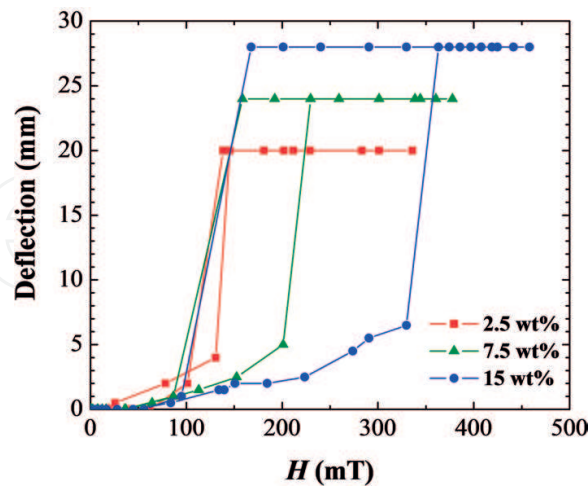
Figure 11. Hysteresis loops of the deflection versus electric current (proportional to the magnetic field) for ferrogels with different concentrations of Fe₃O₄ microparticles: 2.5 wt%, 7.5 wt%, and 15 wt%.

9. Conclusions

PVA hydrogel and ferrogels with Fe$_3$O$_4$ micro- and nano-sized particles as fillers have been successfully prepared by freezing-thawing (F-T) cyclic method. We can conclude the chapter as the following:

- In the biomedical application, a study of hydrogen (water molecules) diffusion behavior in the PVA hydrogel by analyzing the ADC value can be used as a parameter of brain tumor grading. The b-value of 1000 s/mm^2 and higher providing a better image quality and contrast is recommended for brain tumor grading.

- The time dependence of the elongation and deflection curves as a function of PVA concentration, particle concentration, and a number of F-T cycles can be used to determine the durability and performance of the ferrogel under certain external magnetic fields. It has been suggested that ferrogel with PVA and water ratio of 23:100 and four times F-T cycles, respectively, has the best elastic properties. Ferrogel fabricated by a F-T cyclic process has the best magnetoelastic response when it has a relatively large magnetic particle size as the filler with a concentration of 10–15 wt% in the PVA hydrogel.

Acknowledgements

Author details

Malik Anjelh Baqiya[1], Ahmad Taufiq[2], Sunaryono[2], Munaji[3], Dita Puspita Sari[1], Yanurita Dwihapsari[1] and Darminto[1]*

*Address all correspondence to: darminto@physics.its.ac.id

1 Department of Physics, Faculty of Mathematics and Natural Sciences, Institut Teknologi Sepuluh Nopember (ITS), Kampus ITS Keputih Sukolilo, Surabaya, Indonesia

2 Department of Physics, Faculty of Mathematics and Natural Sciences, Universitas Negeri Malang, Malang, Indonesia

3 Faculty of Engineering, Universitas Muhammadiyah Ponorogo, Ponorogo, Indonesia

References

[1] Ullah F, Othman MBH, Javed F, Ahmad Z, Akil HM. Materials Science and Engineering: C. 2015;**57**:414

[2] Caló E, Khutoryanskiy VV. European Polymer Journal. 2015;**65**:252

[3] Gyles DA, Castro LD, Silva JOC, Ribeiro-Costa RM. European Polymer Journal. 2017; **88**:373

[4] Hamidi M, Azadi A, Rafiei P. Advanced Drug Delivery Reviews. 2008;**60**:1638

[5] Priya James H, John R, Alex A, Anoop KR. Acta Pharmaceutica Sinica B. 2014;**4**:120

[6] Bastiancich C, Danhier P, Préat V, Danhier F. Journal of Controlled Release. 2016;**243**:29

[7] Hennink WE, van Nostrum CF. Advanced Drug Delivery Reviews. 2012;**64**(Supplement, 223)

[8] Akhtar MF, Hanif M, Ranjha NM. Saudi Pharmaceutical Journal. 2016;**24**(5):554

[9] Ahmed EM. Journal of Advanced Research. 2015;**6**:105

[10] Qiu Y, Park K. Advanced Drug Delivery Reviews. 2012;**64**(Supplement, 49)

[11] Koetting MC, Peters JT, Steichen SD, Peppas NA. Materials Science and Engineering: R: Reports. 2015;**93**:1

[12] Schwall CT, Banerjee IA. Materials. 2009;**2**:577

[13] Hoare TR, Kohane DS. Polymer. 2008;**49**:1993

[14] Stauffer SR, Peppast NA. Polymer. 1992;**33**:3932

[15] Hassan CM, Peppas NA. Biopolymers PVA Hydrogels, Anionic Polymerisation Nano-composites. Berlin Heidelberg, Berlin, Heidelberg: Springer; 2000. p. 37

[16] Ricciardi R, Auriemma F, De Rosa C, Lauprêtre F. Macromolecules. 2004;**37**:1921

[17] Ricciardi R, Auriemma F, Gaillet C, De Rosa C, Lauprêtre F. Macromolecules. 2004;**37**:9510

[18] Hernandez R, Lopez D, Mijangos C, Guenet J-M. Polymer. 2002;**43**:5661

[19] Hernández R, Sarafian A, López D, Mijangos C. Polymer. 2004;**45**:5543

[20] Park J-S, Park J-W, Ruckenstein E. Journal of Applied Polymer Science. 2001;**82**:1816

[21] Li Y, Hu Z, Chen Y. Journal of Applied Polymer Science. 1997;**63**:1173

[22] Gupta S, Webster TJ, Sinha A. Journal of Materials Science: Materials in Medicine. 2011; **22**:1763

[23] Siddhi G, Sudipta G, Arvind S. Biomedical Materials. 2012;**7**, 015006

[24] Fumio U, Hiroshi Y, Kumiko N, Sachihiko N, Kenji S, Yasunori M. International Journal of Pharmaceutics. 1990;**58**:135

[25] Jiang S, Liu S, Feng W. Journal of the Mechanical Behavior of Biomedical Materials. 2011;**4**:1228

[26] Armas AF, Gonzalez JS, Maiolo AS, Hoppe CE, Alvarez VA. Procedia Materials Science. 2012;**1**:483

[27] Liu T-Y, Hu S-H, Liu T-Y, Liu D-M, Chen S-Y. Langmuir. 2006;**22**:5974

[28] Liu T-Y, Hu S-H, Liu K-H, Liu D-M, Chen S-Y. Journal of Controlled Release. 2008;**126**:228

[29] Liu Y, Vrana NE, Cahill PA, McGuinness GB. Journal of Biomedical Materials Research Part B: Applied Biomaterials. 2009;**90B**:492

[30] Vrana NE, O'Grady A, Kay E, Cahill PA, McGuinness GB. Journal of Tissue Engineering and Regenerative Medicine. 2009;**3**:567

[31] Jiang S, Su Z, Wang X, Liu S, Yu Y. Materials Science and Engineering: C. 2013;**33**:3768

[32] Yanagawa F, Sugiura S, Kanamori T. Regenerative Therapy. 2016;**3**:45

[33] Forte AE, Galvan S, Manieri F, Rodriguez F, Baena Y, Dini D. Materials & Design. 2016;**112**:227

[34] Gonzalez JS, Hoppe CE, Muraca D, Sánchez FH, Alvarez VA. Colloid and Polymer Science. 2011;**289**:1839

[35] Sivudu KS, Rhee KY. Colloids and Surfaces A: Physicochemical and Engineering Aspects. 2009;**349**:29

[36] Martínez H, D'Onofrio L, González G, in LACAME 2012: Proceedings of the 13th Latin American Conference on the Applications of the Mössbauer Effect, (LACAME 2012) held in Medellín, Colombia, November 11-16, 2012. edited by C. A. B. Meneses et al. Netherlands, Dordrecht: Springer; 2014. p. 93

[37] Torre B, Bertoni G, Fragouli D, Falqui A, Salerno M, Diaspro A, Cingolani R, Athanassiou A. Scientific Reports. 2011;**1**:202

[38] Weeber R, Kantorovich S, Holm C. The Journal of Chemical Physics. 2015;**143**, 154901

[39] Zrínyi M, Barsi L, Büki A. Polymer Gels and Networks. 1997;**5**:415

[40] Ramanujan RV, Lao LL. Smart Materials and Structures. 2006;**15**:952

[41] Reséndiz-Hernández PJ, Rodríguez-Fernández OS, García-Cerda LA. Journal of Magnetism and Magnetic Materials. 2008;**320**, e373

[42] Hernandez R, Sacristan J, Nogales A, Fernandez M, Ezquerra TA, Mijangos C. Soft Matter. 2010;**6**:3910

[43] Goiti E, Salinas MM, Arias G, Puglia D, Kenny JM, Mijangos C. Polymer Degradation and Stability. 2007;**92**:2198

[44] Zubarev A. Physica A: Statistical Mechanics and its Applications. 2013;**392**:4824

[45] Zubarev AY, Elkady AS. Physica A: Statistical Mechanics and its Applications. 2014;**413**:400

[46] Zubarev AY, Borin DY. Journal of Magnetism and Magnetic Materials. 2015;**377**:373

[47] Moscoso-Londoño O, Gonzalez JS, Muraca D, Hoppe CE, Alvarez VA, López-Quintela A, Socolovsky LM, Pirota KR. European Polymer Journal. 2013;**49**:279

[48] Sunaryono A, Taufiq EGR, Putra A, Okazawa I, Watanabe N, Kojima S, Rugmai S, Soontaranon M, Zainuri, Triwikantoro S, Pratapa, Darminto. Nano. 2016;**11**, 1650027

[49] Sunaryono A, Taufiq, Munaji B, Indarto, Triwikantoro M, Zainuri, Darminto. AIP Conference Proceedings. 2013;**1555**:53

[50] Dwihapsari Y, Sari DP, Darminto. AIP Conference Proceedings. 2012;**1454**:53

[51] Sari DP, Kristanto SA, Wahyudi RE, Dwihapsari Y, Darminto: In Instrumentation, Communications, Information Technology, and Biomedical Engineering (ICICI-BME), 2013 3rd International Conference on 2013. p. 302

[52] Triwikantoro MA, Baqiya T, Heriyanto, Mashuri, Darminto. Journal of Superconductivity and Novel Magnetism. 2017;**30**:555

[53] Baqiya MA, Taufiq A, Sunaryono K, Ayun M, Zainuri S, Pratapa, Triwikantoro, Darminto: In: Magnetic Spinels- Synthesis, Properties and Applications, edited by Seehra MS. Rijeka: InTech; 2017. p. Ch. 11

[54] Moritani T, Ekholm S, Westesson P-L. Diffusion-Weighted MR Imaging of the Brain. 2nd ed. New York: Springer; 2009

[55] Seo HS, Chang K-H, Na DG, Kwon BJ, Lee DH. American Journal of Neuroradiology. 2008;**29**:458

[56] Hassan CM, Ward JH, Peppas NA. Polymer. 2000;**41**:6729

[57] Amsden B. Macromolecules. 1998;**31**:8382

[58] Fromageau J, Gennisson J, Schmitt C, Maurice R, Mongrain R, Cloutier G. IEEE Transactions on Ultrasonics, Ferroelectrics, and Frequency Control. 2007;**54**:498

[59] Zrínyi M, Barsi L, Szabó D, Kilian H-G. The Journal of Chemical Physics. 1997;**106**:5685

[60] Snyder RL, Nguyen VQ, Ramanujan RV. Acta Materialia. 2010;**58**:5620

[61] Morozov K, Shliomis M, Yamaguchi H. Physical Review E. 2009;**79**:040801

[62] Puspitasari T, Raja KML, Pangerteni DS, Patriati A, Putra EGR. Procedia Chemistry. 2012;**4**:186